

Spatiotemporal Behavior of Drift Waves in LMD-U

Takuma YAMADA, Sanae -I. ITOH, Kenichiro TERASAKA¹⁾, Naohiro KASUYA²⁾, Yoshihiko NAGASHIMA, Shunjiro SHINOHARA¹⁾, Takashi MARUTA¹⁾, Masatoshi YAGI, Shigeru INAGAKI, Yoshinobu KAWAI, Akihide FUJISAWA²⁾ and Kimitaka ITOH²⁾

Research Institute for Applied Mechanics, Kyushu University, Kasuga 816-8580, Japan

¹⁾*Interdisciplinary Graduate School of Engineering Sciences, Kyushu University, Kasuga 816-8580, Japan*

²⁾*National Institute for Fusion Science, Toki 509-5292, Japan*

(Received 10 November 2007 / Accepted 17 February 2008)

In the LMD-U linear magnetized plasma, fluctuation measurements have been performed with multi-channel poloidal Langmuir probe arrays to investigate the spatiotemporal behaviors of drift wave turbulence. Two-dimensional (poloidal mode number–frequency) power spectrum showed not only fluctuation peaks but also the existence of a broadband fluctuation. The broadband fluctuation developed at high poloidal mode number and high frequency regions and not along the linear dispersion relation curve of drift wave modes. It showed shorter correlation time and poloidal length than the peaked fluctuations. Two-dimensional axial coherence was measured with two poloidal probe arrays separated in the axial direction. The axial coherence was strong for both the broadband fluctuation and peak fluctuations, suggesting the quasi-two-dimensional structure of the drift wave turbulence.

© 2008 The Japan Society of Plasma Science and Nuclear Fusion Research

Keywords: linear plasma, drift wave, turbulence, broadband fluctuation, quasi-two-dimensional structure

DOI: 10.1585/pfr.3.S1021

1. Introduction

Recently, there has been an advance in the study of the nonlinear interaction between drift wave turbulence and meso-scale structures such as zonal flows and streamers [1, 2], and experiments in linear plasma devices have been in progress [3–10]. In these studies, complex wave patterns in poloidal direction have been observed (see also reports from toroidal plasma experiments, e.g., [11–14]). These advancements highlight the need to measure fluctuations at multiple spatial positions simultaneously. Fluctuation measurements have been performed with poloidal multi-probe arrays in linear and toroidal plasmas [3, 4, 6, 15].

In the LMD-U linear magnetized plasma [16], multi-point measurements of the ion saturation-current and floating potential fluctuations are in progress with poloidal Langmuir probe arrays. Drift wave modes driven by steep radial density gradient were identified, and a drift wave turbulence regime was achieved [17]. The poloidal mode numbers and frequencies of the drift wave modes were compared with the calculated linear dispersion relation of drift wave [18], and they were in a good agreement. Moreover, in a drift wave turbulence regime, quasi-modes and broadband components that do not satisfy the dispersion relation were found. They were considered to be produced by nonlinear couplings of primary modes [19]. In the previous works, the details of the broadband components were not reported, while the quasi-modes were discussed in detail. In this article, we report the detailed characters of the

broadband components found in the drift wave turbulence regime. In particular, the reported axial correlation measurement with two poloidal probe arrays is a new analysis method.

2. Poloidal Probe Arrays

We have performed a quasi-two-dimensional measurement of the ion saturation-current fluctuation of the LMD-U linear plasma [16]. The schematic view of the LMD-U device is shown in Fig. 1. A linear magnetized plasma is created by an rf wave (frequency = 7 MHz and power = 3 kW) in a quartz tube (axial length = 0.4 m and inner diameter = 0.095 m) with argon gas filled in. The plasma is guided along a linear magnetic field created by magnetic coils surrounding the vacuum vessel to form a column shape. The axial length and inner diameter of the vacuum vessel are 3.74 m and 0.445 m, respectively.

There are two poloidal Langmuir probe arrays installed in LMD-U. A 64-channel poloidal probe array is installed at an axial position of 1.885 m, and a 48-channel poloidal probe array is installed at 1.625 m. The tungsten probe tips of the 64-channel probe array are fixed at the measuring radius of 40 mm (the probe tips are 3.9 mm apart), and the position of the whole probe array is adjustable two-dimensionally in the plasma cross section. Therefore, the precise measurement of the poloidal mode number of the fluctuation is possible with this probe array [20]. The 48-channel probe array consists of 16 probe units, which are movable in the radial direction. Each

author's e-mail: takuma@riam.kyushu-u.ac.jp

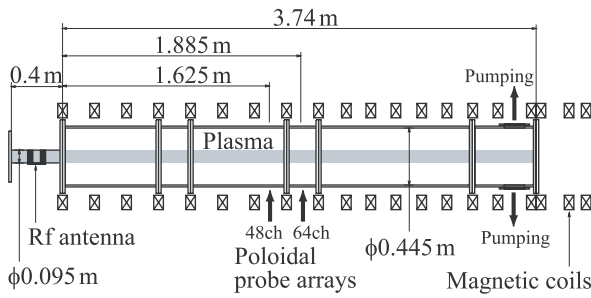


Fig. 1 Schematic view of the LMD-U linear plasma device and positions of poloidal arrays (64-channel and 48-channel).

probe unit has 3 tungsten probe tips. The probe tips are arranged at an equal distance when the measuring radius is set to 40 mm (the probe tips are 5.2 mm apart). This probe array can measure the poloidal mode number and radial profile of the plasma fluctuation [17]. With these two poloidal probe arrays, the details of the broadband and peak fluctuations, such as poloidal mode numbers, poloidal correlation lengths, and axial correlations, which are functions of mode number and frequency, are measurable.

3. Spectral Analysis

By changing the discharge condition, the spatiotemporal behavior of the ion saturation-current fluctuation varies from a periodically, coherent wave structure to a turbulence regime, which consists of many fluctuation components with different poloidal mode numbers and frequencies [4]. In LMD-U, increasing the magnetic field (over 0.04 T) and decreasing the argon pressure (under 0.4 Pa) change the plasma into the turbulence regime by affecting the density gradient and collision with neutrals [16]. Figure 2 shows the spatiotemporal behavior of the ion saturation-current $I(\theta, t)$, where θ is the poloidal angle and t is the time, in the turbulence regime measured with the 64-channel probe array. The magnetic field was 0.09 T and the argon pressure was 0.27 Pa. The increasing direction of the poloidal angle θ corresponds to the electron diamagnetic direction. The spatiotemporal waveform consists of a number of fluctuation components. The main fluctuation is the propagation in the electron diamagnetic direction with a frequency of about 3 kHz.

The spatiotemporal waveform in the turbulence regime can be decomposed into the poloidal mode number (m) and frequency (f) spaces by spectral analysis. By two-dimensional Fourier transformation, $I(\theta, t)$ is transformed to $\hat{I}(m, f)$. Figure 3 shows the power spectrum $S(m, f) = \langle |\hat{I}(m, f)|^2 \rangle / df$, where df is the frequency resolution and is 0.1 kHz in this case. The power spectrum $S(m, f)$ is an ensemble of 300 time windows with 10-ms ($= df^{-1}$) length. One of the advantages of poloidal multi-point detection over single point measurement is that the poloidal propagating direction can be determined in the

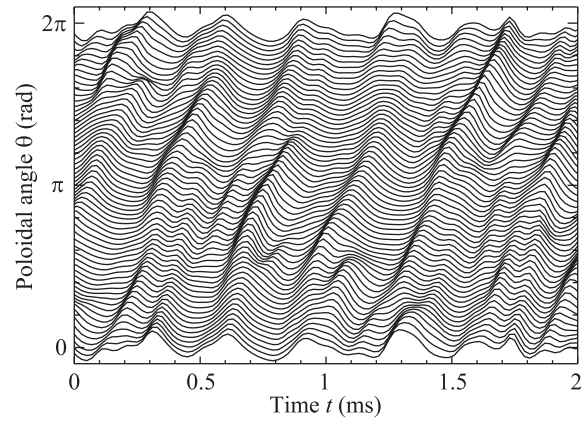


Fig. 2 Spatiotemporal behavior of ion saturation-current $I(\theta, t)$ measured with the 64-channel poloidal probe array.

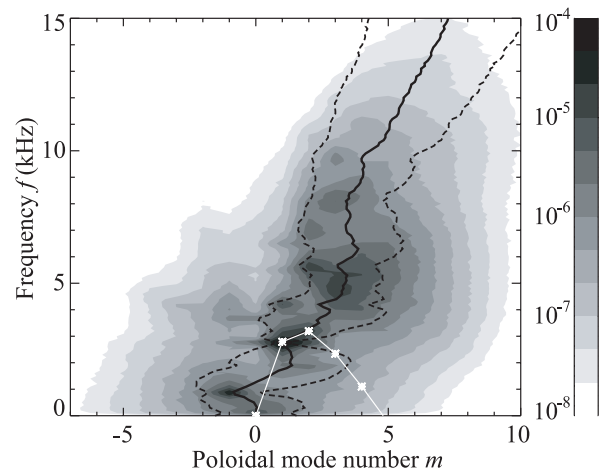


Fig. 3 Contour plot of power spectrum $S(m, f)$ (arb. unit) plotted over calculated linear dispersion relation of drift waves (white asterisks). Solid black line shows mean poloidal mode number, and broken black lines show spread of the mode number.

former. When frequency is set to $f \geq 0$, fluctuations with positive and negative poloidal mode numbers propagate in the electron and ion diamagnetic directions, respectively.

The white asterisks in Fig. 3 show the calculated linear dispersion relation of drift waves with a uniform rotation assuming a dc radial electric field. The value of the electric field (30 V/m) was selected as the strongest peak at $(m, f) = (1, 2.8 \text{ kHz})$ to match the eigenfrequency, and was within an error-bar of the potential profile measurement [19]. The peak at $(m, f) = (2, 3.2 \text{ kHz})$ also satisfies the dispersion relation. The peak at $(m, f) = (-1, 0.9 \text{ kHz})$ is a flute wave-like mode in the ion diamagnetic direction. Other fluctuation peaks such as $(m, f) = (2, 5.6 \text{ kHz})$ and $(3, 4.7 \text{ kHz})$ do not satisfy the dispersion relation, and they are quasi-modes. The solid and broken lines in Fig. 3 show the frequency dependences of the mean poloidal mode number and the spread of the mode number, respectively. They are

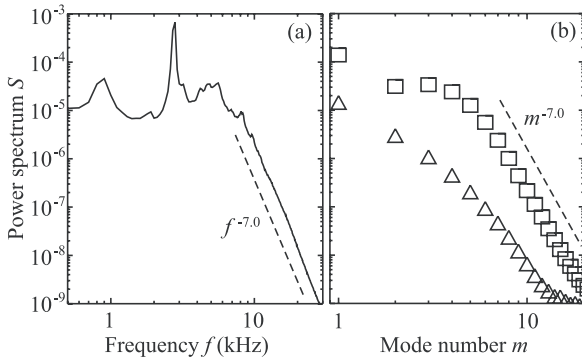


Fig. 4 One-dimensional power spectra (a) $S(f)$ and (b) $S(m)$ (squares) and $S(-m)$ (triangles) (arb. unit). Dashed lines show relationships $S \propto f^{-7.0}$ and $S \propto m^{-7.0}$.

defined as

$$\langle m(f) \rangle = \frac{\sum_m m S(m, f)}{\sum_m S(m, f)}, \quad (1)$$

$$\Delta m(f)^2 = \frac{\sum_m [m - \langle m(f) \rangle]^2 S(m, f)}{\sum_m S(m, f)}. \quad (2)$$

The mean poloidal mode number traces the strong fluctuation peaks, and the spread decreases if strong peaks exist. In the high frequency region with no remarkable fluctuation peaks ($f > 10$ kHz), the mean poloidal mode number increases with the relationship $\langle m \rangle \propto f$ and the spread is an increasing function of f . These facts imply the existence of broadband components. The quasi-mode peaks and broadband components appear nearly on the line $\langle m \rangle \propto f$, and they are away from the linear dispersion relation curve of the drift wave, irrespective of the value of the radial electric field. Quasi-modes and broadband components are considered to be produced by nonlinear couplings of parent modes [19].

Figure 4 shows the logarithmic plots of power spectra $S(f)$ and $S(m)$ calculated by integrating $S(m, f)$ with m and f , respectively. Both spectra have relations $S(f) \propto f^{-7.0}$ and $S(m) \propto m^{-7.0}$ in broadband regions ($f > 10$ kHz or $m > 5$). It is interesting that the decay laws are identical in the frequency and poloidal mode number spaces. It is also interesting that the power law of $S(m)$ is nearly equal to that obtained from a previous study [i.e., $S(m)^{0.5} \propto m^{-3.6}$ [3]]. Although different experimental conditions induce individual eigenfunctions, the power laws in broadband regions become almost identical.

4. Broadband Fluctuation

The details of the broadband fluctuation were explored. First, the lifetime of the broadband fluctuation was investigated. Figure 5 shows the auto-correlation functions of the ion saturation-current fluctuation in the frequency ranges of full-range and $f > 10$ kHz. Owing to the main

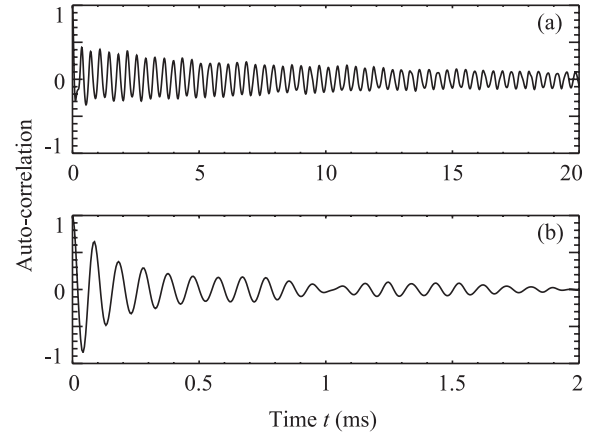


Fig. 5 Auto-correlation functions of ion saturation-current fluctuation in the frequency ranges of (a) full-range and (b) broadband region ($f > 10$ kHz).

peak fluctuations, the auto-correlation time of the former (full-range) is long (about the order of 10 ms). On the other hand, the auto-correlation time of the latter ($f > 10$ kHz, which is in the broadband region), is short (about the order of 1 ms). It means that the broadband fluctuation has a shorter lifetime than the main peak fluctuations. Several short time fluctuations with various frequencies accumulate to form a broadband fluctuation.

Second, correlation length (poloidal angle) was calculated from the 64-channel data. Coherence coh of two time data I_x and I_y is defined by

$$coh^2(f) = \frac{|S_{xy}(f)|^2}{S_{xx}(f)S_{yy}(f)}, \quad (3)$$

where $S_{xy} = \langle \hat{I}_x \hat{I}_y^* \rangle / df$ and asterisk indicates complex conjugate. Correlation length is the distance where the coherence becomes e^{-1} . Figure 6 shows the frequency dependence of the coherence in the poloidal angle space. To obtain Fig. 6, the signal of the channel at $\theta = 0$ was used as x , and all the signals of the 64 channels were used as y , which was taken along the horizontal axis. The correlation lengths in the poloidal direction are long for peak fluctuations such as 0.9 and 2.8 kHz, and are short (under $\pi/4$) for broadband components. The correlation length decreases gradually as the frequency increases. From this result, strong fluctuation peaks are produced globally in the poloidal direction, while broadband components are produced locally in the poloidal direction.

Third, the axial correlation was analyzed with the poloidal probe arrays. One of the features of our experiment is that two poloidal probe arrays are used for fluctuation measurements; therefore, a quasi-two-dimensional measurement is available. By setting all of the measuring radii of the 48-channel probe array tips to 40 mm, poloidal analyses of the plasma column in separate lengths of 0.26 m in the axial direction are performed. The 64-channel probe array can measure the poloidal mode num-

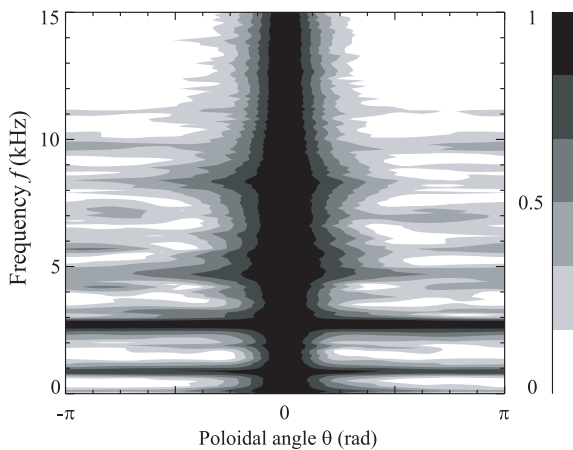


Fig. 6 Frequency dependence of coherence in poloidal angle space. Correlation lengths are long for fluctuation peaks and short for broadband components.

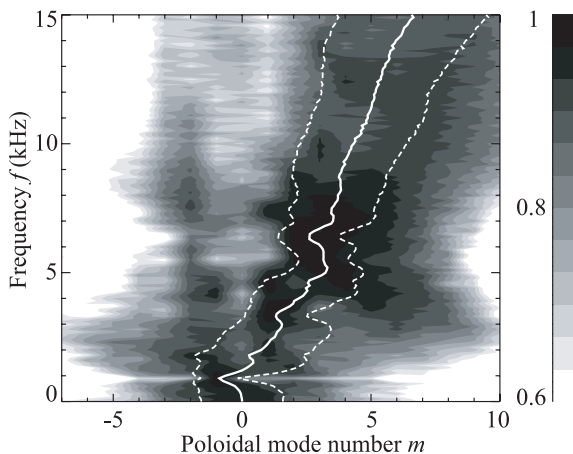


Fig. 7 Axial coherence between two poloidal probe arrays in m - f space. Coherences are strong not only for fluctuation peaks but also for broadband components. Solid white line shows mean poloidal mode number (which is shown in Fig. 3), and broken white lines show spread of the mode number.

ber $|m| \leq 32$, and the 48-channel probe array can measure $|m| \leq 24$. Since the two probe arrays have different numbers of probes, many of the poloidal positions of them do not agree. However, the fluctuations of the poloidal mode number in the region $|m| \leq 24$ can be compared, and axial correlations unfolded in the m - f space can be calculated. The detailed axial behaviors of the measured fluctuations are available by this new technical method. Figure 7 shows the coherence between the two poloidal probe arrays in the poloidal mode number–frequency space. Compared with Fig. 3, it can be said that the coherences are strong not only for the fluctuation peaks such as drift wave modes, but also for broadband components even though the spectral powers are small. This fact suggests quasi-two-dimensional characteristics of the magnetized plasma turbulence.

5. Summary

In summary, we have performed a measurement of drift wave turbulence in the LMD-U linear magnetized plasma with two poloidal probe arrays. The obtained two-dimensional power spectrum $S(m, f)$ showed excitation of not only fluctuation peaks, but also broadband components ($\langle m \rangle \propto f$ and $S \propto f^{-7.0}, m^{-7.0}$), which do not satisfy the linear dispersion relation of drift wave modes. The details of the broadband components were investigated by the probe arrays. The correlation time of the broadband fluctuation was shorter than those of the peak fluctuations. The correlation lengths in the poloidal direction were short (under $\pi/4$) for broadband components, and suggested that these fluctuations were produced locally in the poloidal direction. Axial coherence between the two poloidal probe arrays was calculated in the m - f space, and showed that the broadband and peaked fluctuations had strong axial coherences, i.e., the plasma had a quasi-two-dimensional structure.

Acknowledgments

This work was supported by a Grant-in-Aid for Specially-Promoted Research of MEXT (16002005) (Itoh Project), Grant-in-Aid for Young Scientists (B) of JSPS (19760597), and the collaboration programs of NIFS (NIFS07KOAP017) and RIAM, Kyushu University.

- [1] P.H. Diamond *et al.*, *Plasma Phys. Control. Fusion* **47**, R35 (2005).
- [2] A. Yoshizawa, S.-I. Itoh and K. Itoh, *Plasma and Fluid Turbulence, Theory and Modelling* (Institute of Physics Publishing, Bristol and Philadelphia, 2003).
- [3] A. Latten, T. Klinger and A. Piel, *Rev. Sci. Instrum.* **66**, 3254 (1995).
- [4] T. Klinger *et al.*, *Phys. Rev. Lett.* **79**, 3913 (1997).
- [5] M. Kono and M.Y. Tanaka, *Phys. Rev. Lett.* **84**, 4369 (2000).
- [6] C. Schröder *et al.*, *Phys. Rev. Lett.* **86**, 5711 (2001).
- [7] T. Kaneko, H. Tsunoyama and R. Hatakeyama, *Phys. Rev. Lett.* **90**, 125001 (2003).
- [8] V. Sokolov and A.K. Sen, *Phys. Rev. Lett.* **92**, 165002 (2004).
- [9] M.J. Burin *et al.*, *Phys. Plasmas* **12**, 052320 (2005).
- [10] G.R. Tynan *et al.*, *Plasma Phys. Control. Fusion* **48**, S51 (2006).
- [11] C. Lechte, S. Niedner and U. Stroth, *New J. Phys.* **4**, 34 (2002).
- [12] Y. Nagashima *et al.*, *Phys. Rev. Lett.* **95**, 095002 (2005).
- [13] Y. Hamada *et al.*, *Phys. Rev. Lett.* **96**, 115003 (2006).
- [14] F.M. Poli *et al.*, *Phys. Plasmas* **13**, 102104 (2006).
- [15] U. Stroth *et al.*, *Phys. Plasmas* **11**, 2558 (2004).
- [16] S. Shinohara *et al.*, *Proc. 28th Int. Conf. on Phenomena in Ionized Gases* (Institute of Plasma Physics AS CR, Prague, 2007), 1P04-08.
- [17] K. Terasaka *et al.*, *Plasma Fusion Res.* **2**, 031 (2007).
- [18] N. Kasuya *et al.*, *J. Phys. Soc. Jpn.* **76**, 044501 (2007).
- [19] T. Yamada *et al.*, *Plasma Fusion Res.* **2**, 051 (2007).
- [20] T. Yamada *et al.*, *Rev. Sci. Instrum.* **78**, 123501 (2007).